

Modelization of the bonding process for a non-woven fabric: analysis and numerics

F. Bagagiolo¹, E. Bertolazzi², L. Marzufero³, A. Pegoretti², D. Rigotti²

¹Department of Mathematics, University of Trento, Italy

²Department of Industrial Engineering, University of Trento, Italy

³Faculty of Economics and Management, Free University of Bozen-Bolzano, Italy

Abstract

We are concerned with the study and the research developed at the University of Trento about a problem posed by the company Fater S.p.A., in Italy. Such a problem consists in a possible analysis of the behavior of the bonding process of a non-woven fabric. In particular, the bonding process is not given by the use of some kind of glue, but just by the pressure of two fiber webs through two high-velocity steel-made rollers. The aim of such a process is to produce diaper linings. The research comprised the formulation and theoretical as well as numerical analysis of analytical, mechanical and thermal models for the stress-strain behavior of the non-woven fabric's fibers and for the bonding process with heating effects.

Keywords: non-woven fabric; bonding process modeling; heat equation; numerical simulation.

AMS subject classification: 65L05; 65M06; 80A19; 80M20.

1. Introduction

A non-woven fabric is a manufactured material made from polymer fibers which are bonded together through industrial processes that usually involve pressure and heating effects. There are several purposes for the use of nonwoven fabrics, such as medical fabrics, filters, or geotextile ones. Among them, we can also find the use for the production of diaper linings. The paper is indeed concerned with the modelization of a bonding process for a non-woven fabric used for the manufacturing of diapers. In particular, the problem was posed by the Italian company Fater S.p.A, specialized in the market of absorbent products, with the aim of a better understanding of their industrial bonding process for producing diapers, in the event that the nonwoven fabric is provided with different physical and mechanical parameters. Such a bonding process performed by the company does not require the use of some kind of glue but involves just the pressure of two fabric webs passing through two high-velocity steel-made rollers that compress them. In this way, an instantaneous heat diffusion and local fusing effect take place and the two webs of non-woven fabric will get glued. The mechanics behind this kind of bonding process is also partly shared by the bonding process used to produce a non-woven fabric; see [1,2] for more details. Our purpose is then to model the bonding process, both from an analytical and numerical point of view, as a function of the compression and the velocity of the rollers. To this aim, two different models for the heat diffusion were studied, a linear and a parabolic one. The first is less accurate and involves just ordinary linear differential equations for temperature (see [3]), whereas the second aims to enhance the compression of the fusing process by exploiting the heat equation (see [4]).

As regards the experimental part, the use of laboratories and equipments, we made use of the expertise of some of the authors who have already worked on similar models as in [5]. See also the references therein for the industrial importance of such materials.

This allows us to study the behavior of the resulting diaper lining even in the case some parameters like thickness are different. Our investigation is detailed as in the following sections.

In Section 2, we briefly describe the non-woven fabric, the way it is usually produced and the intended use. Some pictures (made by an electronic microscope) of the non-woven fabric used by the company are reported. In particular, such pictures clearly enlighten the fact that the bonding process exploited for the production of the fabric presents an evident thermal effect. The following chapters will then study from

an analytical, mechanical and numerical point of view a new model taking into account those thermal effects.

In Section 3, after our laboratory experiments, we get that the thermal effect, i.e. the temperature increment of the non-woven fabric, is due to the almost instantaneous compression process. We then collect other experimental results as well as data from literature in order to precisely fit the nature of the fabric and estimate the involved parameters, such as specific heat, Young's modulus, etc. Thereafter, some analytical models inspired by the so-called heat equation are formulated and studied.

In Section 4, we further specify the analytical model in Section 3, making it more suitable for the real process of compression and bonding given by the passage of the fabric webs through the rollers. Then a one-dimensional and a bi-dimensional numerical model and the relative numerical results are reported. In particular, such results clearly show the patterns of effective thermally bonding as function of the compression of the fabric and of the velocity of the assembly line.

2. Description of the non-woven fabric

A non-woven fabric is a fabric-like material produced by bonding together staple short or continuous long fibers through chemical or mechanical processes. Many treatments for producing non-woven fabrics exist. For example, one can apply heat and pressure for bonding at limited areas of a non-woven film by passing it through the nip between heated calendar rolls either or both of which may have patterns of lands and depressions on their surfaces. During such a bonding process, depending of the types of fibers making up the non-woven film, the bonded regions may be formed independently of external influence or aid, i.e. the fibers of the film are melt fused at least in the pattern areas or with the addition of an adhesive. The advantages of thermally bonded non-woven fabrics include low energy costs and speed of production.

Non-woven fabrics can also be made by other processes. For more details see the patents [1] and [2] and references (and other patents) therein. However, in all of the non-woven fabrics, the producing process usually realizes punched rigid spots on the pattern giving them a sort of frame. For simplicity, from now on such punched rigid spots will be called *tags*.

The non-woven fabric provided by the company is used for producing diapers linings and is formed by polypropylene. Generally, non-woven fabrics are also used for medical and sanitary stuff like hospital gowns, wipes and masks and may be also formed by other types of polymers, like polyolefin and polyester. In particular, the company exploits a further bonding process to thermally bond pieces of raw non-woven fabric (made in turn by a bonding process like the ones described above) in order to build pieces of a diaper lining. The technical equipment used for such a bonding process is patented by the company and very similar to the one in [2]: two fiber webs pass through a pair of high velocity steel-made rollers which thermally fuse them in the pattern areas by applying a suitable almost instantaneous pressure. In principle, no heating process is needed for the rollers (for more details, see the Section 4). Therefore, the description of the production suggests the numerical modelization of the bonding process.

2.1. First collection of pictures

In this section, we report some pictures of pieces of the non-woven fabric provided by the company, made by Heerbrugg Wild M3Z optical microscope, without any focus on the thermally bonded pattern. The presence of tags and the fibers is shown anyway.

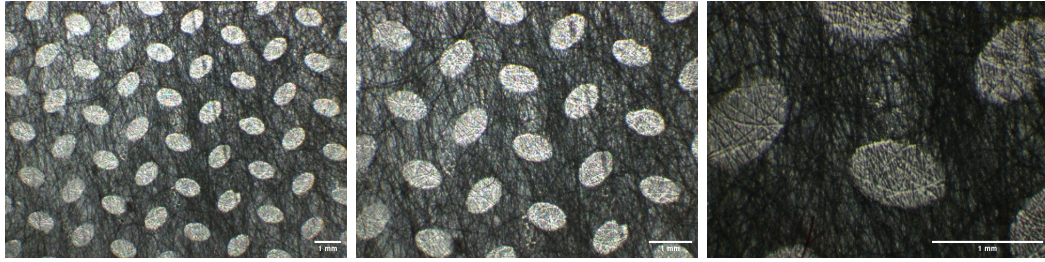


Figure 1. First collection of pictures: you can see the elliptic shape of the tags and randomness of fibers.

2.2. Second collection of pictures

Here we report another collection of pictures with a detailed focus on the thermally bonded areas, that unequivocally shows that, around the elliptic tags, the almost instantaneous compression process induces a thermal bonding with a resulting local fusing. The microscope we used is Zeiss Supra 40 field emission scanning electron microscope (FESEM), operating at an accelerating voltage of 2.5 kV. A thin platinum palladium conductive coating was deposited on the surface of the samples before the observations.

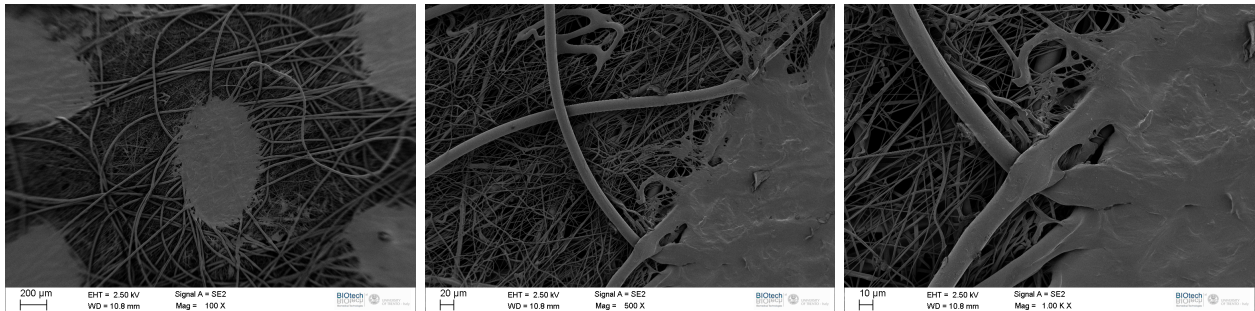


Figure 2. Second collection of pictures: you can see the fused pattern areas near elliptic tags induced by the thermally bonding process.

3. Polypropylene data and modelization

The aim of this section is to compute the temperature increment and the temperature decay of the non-woven fabric through a suitable compression rate. We will provide two models, a linear and a quadratic one. To do that, we will need some data of the fabric, polypropylene and steel, which we will recover a little from the literature and a little from laboratories experiments.

3.1. Tacticity and some data from literature

In order to establish which is the polypropylene's type (atactic, isotactic, syndiotactic) of the non-woven fabric, we performed a spectrum analysis, made with a Fourier transformed infrared (FT-IR) spectrophotometer, using a Avatar 330 by the Thermo Fisher company. The spectrum, as in figure (3), is the result of 64 scans with a resolution of 4 cm^{-1} , and turned out that the polypropylene is atactic.

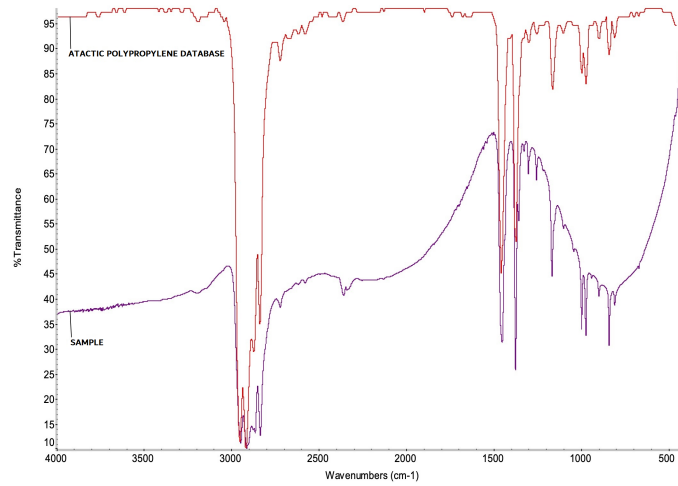


Figure 3. Spectrum comparison of our non-woven fabric with a sample atactic polypropylene.

For the description and the numerical modelization of the bonding process, we need some polypropylene data, that we collect in the following Table 1 (see [6–9]): Due to the high variability of the fusion

Table 1. Physical parameters of polypropylene

Parameter	Value	Unit	
Melting point	130–171	°C	measured 160 °C
Density	855–946	kg/m ³	atactic: 866
Thermal conductivity	0.17–0.22	W/(m K)	at 23 °C typ 0.17
Specific heat	581.97–2884.71	J/(kg K)	temp. in K
Young’s module	1300–1800	N/mm ² = MPa	

temperature 130–171 °C, an accurate measurement is performed at 160 °C. In order to detect that, polypropylene is heated slowly with a constant temperature rate. The heat flux to the polypropylene is measured and, when a negative peak of heat is detected, it means that polypropylene is changing phase from solid to liquid.

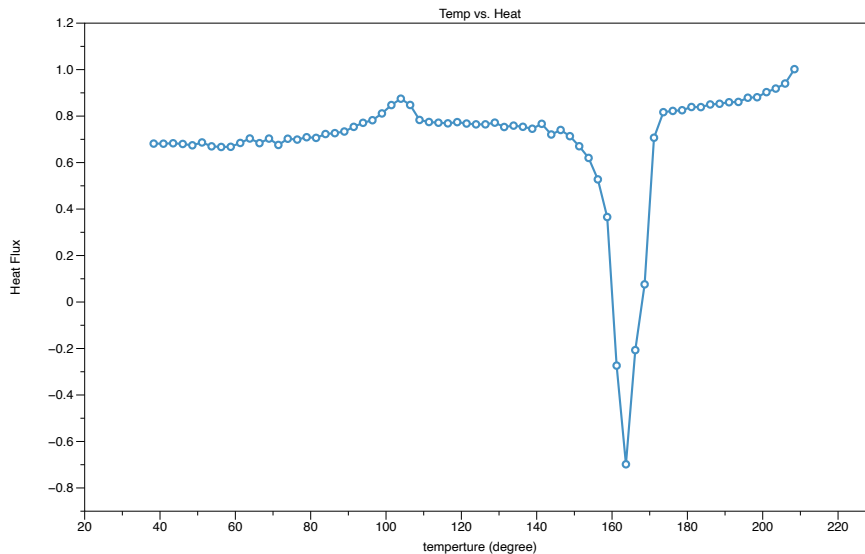


Figure 4. Temperature and heat absorption: the negative peak is the fusion point of the polypropylene, here about 160 °C.

Since the rollers which thermally bond the pieces of non-woven fabric are steel-made, similarly to the polypropylene, we need some physical parameters of the steel, that we collect in the following Table 2 (see [10–13]):

Table 2. Physical parameters of steel

Parameter	Value	Unit
Melting point	1400–1530	°C
Density	7500–8000	kg/m ³
Thermal conductivity (stainless)	15–18	W/(m K)
Thermal conductivity	44–80	W/(m K)
Specific heat	500	J/(kg K)
Young's modulus	180000	N/mm ² = MPa

3.2. Determination of fabric weight by unit area

In this section, we report the density of our non-woven fabric, determined by a 15 cm × 15 cm fabric sample. The next figure shows the fabric piece and its weight, determined by a precision scale Netzsch DSC204.



Figure 5. On the left the precision scale used for the weight determination and on the right the non-woven fabric piece used for the experiment.

It follows that the weight by unit area w_{fabric} is:

$$(1) \quad w_{\text{fabric}} = \frac{[\text{mass}]}{[\text{area}]} = \frac{0.2835 \text{ g}}{150 \text{ mm} \cdot 150 \text{ mm}} = 0.0126 \frac{\text{kg}}{\text{m}^2}.$$

As long as the non-woven fabric is fully compressed, from the density of the polypropylene (see Table 1) we can infer its thickness:

$$h_{\text{fabric}}^{\min} = \frac{[\text{weight}]/[\text{area}]}{[\text{density}]} = \frac{0.0126 \frac{\text{kg}}{\text{m}^2}}{900 \frac{\text{kg}}{\text{m}^3}} = 0.000014 \text{ m} = 0.014 \text{ mm} = 14 \mu\text{m}.$$

3.3. Computation of the thickness: pressure and displacement

In this subsection, we want to establish the thickness of the non-woven fabric not compressed. To do that, we use an indirect approach based on experimental measurements made with the dynamometer Instron 5969, at a speed of 1 mm/min, of the laboratories in the Department of Materials Engineering at the University of Trento.

In particular, at first we characterize the displacement/pressure curve of the dynamometer with the press disk made by seven circle tags without the non-woven fabric. In this way, we determine the offset corresponding to zero thickness to be eliminated in the measurement of the curve. We did two experiments and the results are the following.

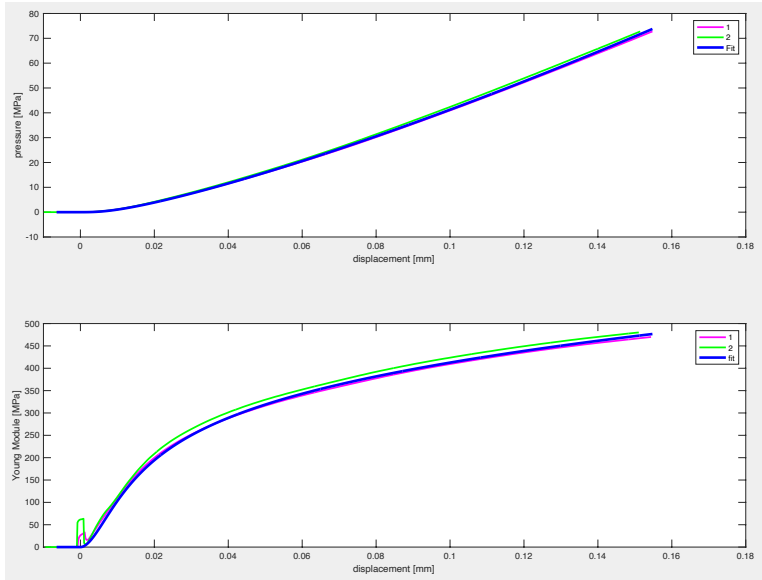


Figure 6. Displacement/pressure graph without the non-woven fabric

The fitting of the pressure is the following

$$P_{\text{base}}(x) = \frac{5461.352911 \max(0, x)^{2.92599}}{0.0038158166 + 6.4490865 \max(0, x)^{1.624481}}$$

After this measurement, ten sheets of non-woven fabric are put under the press disk, getting the following pressure curve.

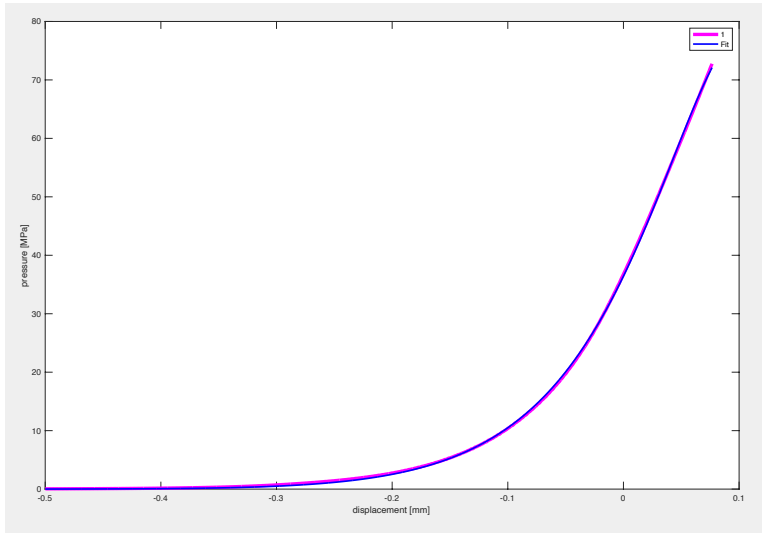


Figure 7. Displacement/pressure graph with ten non-woven fabric sheets

Fitting again the data, we obtain

$$P_{\text{base+10 fabric}}(x) = \frac{716.33893 \max(0, x + 0.9703)^{12.67189680}}{14.10752 + 0.92219399 \max(0, x + 0.9703)^{30.037944}}$$

This shows that the pressure starts growing at $x = -0.9703$ which can be assumed as the thickness of the ten non-woven fabric sheets, and then we can set it to

$$h_{\text{fabric}}^{\max} = \frac{0.97 \text{ mm}}{10} = 97 \mu\text{m}.$$

Due to the very low speed of the displacement movement, the pressures are in equilibrium as follows:

$$P_{\text{base}+10 \text{ fabric}}(x) = P_{\text{base}}(z) = P_{\text{base}}(x - w) = P_{10 \text{ fabric}}(w),$$

where the total displacement $x = z + w$ is the sum of the displacement of the ten non-woven fabric sheets (w) and the press displacement (z). To obtain $P_{10 \text{ fabric}}(w)$, first of all we have to determine x as a function of w by solving

$$(2) \quad P_{\text{base}+10 \text{ fabric}}(x) - P_{\text{base}}(x - w) = 0.$$

This equation can be solved numerically with respect to x and assuming $x(w)$ as known. Then

$$P_{10 \text{ fabric}}(w) = P_{\text{base}+10 \text{ fabric}}(x(w)).$$

The function $x(w)$ is very ill-conditioned and defined for about $w \leq -0.08$. Thus it is better to compute the inverse function $w(x)$ by solving (2) w.r.t. w . Plotting $w(x)/10$ and $P_{\text{base}+10 \text{ fabric}}(x)$, we obtain

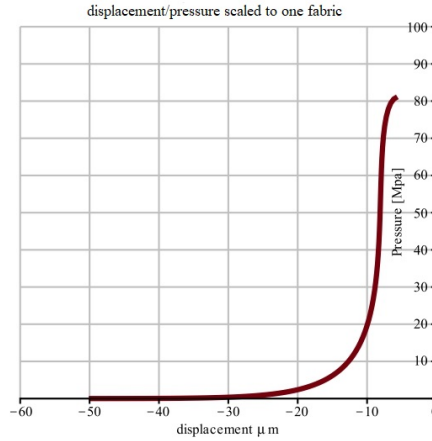


Figure 8. Displacement/pressure graph of a single sheet of non-woven fabric

and this is an approximation of the displacement/pressure curve on a single sheet of non-woven fabric. When the displacement is 0, the fabric has non physical thickness 0 and graph stops at about $-6 \mu\text{m}$. The graph pressure is negligible until displacement is $-30 \mu\text{m}$, and thus we can correct the thickness of the fabric (under mild compression) to $30 \mu\text{m}$.

Hence the fabric under compression at about 5 MPa is fully compressed (the fibers are compacted) and the thickness is about $14 \mu\text{m}$. When pressure grows until 80 MPa , the thickness is reduced to about $7 \mu\text{m}$, and the non-woven fabric assumed as a single block is under a strain of $7/14 = 0.5$. This information will be used to compute the increment of the temperature of the fabric under fast compression.

To make computations workable, we derive from Figure 8 an approximated law linking the strain of the non-woven fabric with the pressure. In Figure 9, a plot of the strain calculated with respect to the compressed fabric and the pressure is fitted with a hyperbolic curve. The x -axis contains the strain:

$$[\text{strain}] = \frac{[\text{displacement}] + h_{\text{fabric}}^{\min}}{h_{\text{fabric}}^{\min}} = \frac{[\text{displacement}] + 14 \mu\text{m}}{14 \mu\text{m}}.$$

Zero strain means that the fabric is fully compressed and positive strain means that the fabric is compressing. Negative strain means that the fabric is not fully compressed and the pressure is relatively low.

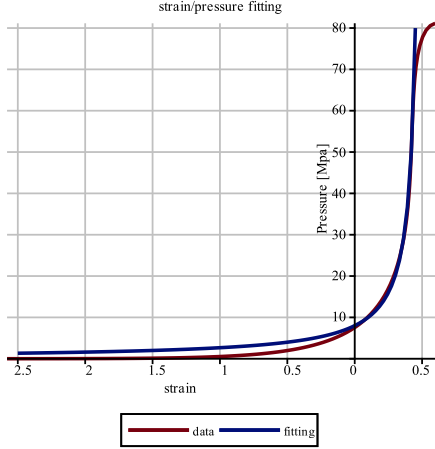


Figure 9. Strain/pressure curve fitting

As you can notice, the pressure in the negative strain part is overestimated, while the positive part is well captured up to a strain of 0.4 (compression of 40%). However, we are interested in the estimation of the heating of the non-woven fabric, and this part of the curve produces a very low effect. The approximated/fitted Young’s modulus becomes

$$(3) \quad \kappa_{\text{fabric}}(s) = \frac{16}{1 - 2s} \quad [\text{MPa}] = \frac{16 \cdot 10^6}{1 - 2s} \quad [\text{Pa}].$$

3.4. Computation of the temperature increment

From the following experimental figure obtained at the University of Trento, it follows that κ_{fabric} (i.e., the Young or Storage modulus) of the non-woven fabric linearly decreases by temperature. Dynamic mechanical analysis (DMA) tests were carried out using a TA Instrument DMA Q800 device, in the temperature range from 25 °C to 120 °C, with a heating rate of 3 °C/min, a strain amplitude of 0.05% and a frequency of 1 Hz. Through this analysis, it was possible to evaluate the Storage modulus, the loss modulus and the loss tangent as a function of the temperature.

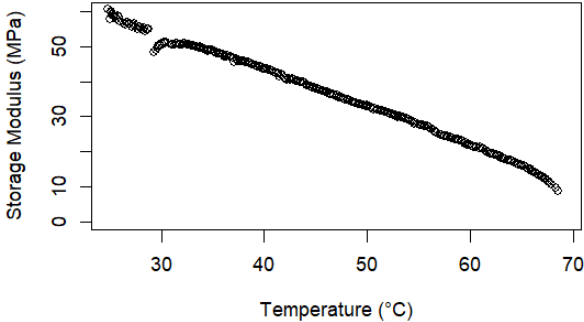


Figure 10. Storage modulus/temperature plot of the non-woven fabric

In particular, the Young modulus linearly decreases from $T_0 = 20 \text{ }^\circ\text{C}$ and reaches 0 at about $90 \text{ }^\circ\text{C}$. The value of the modulus of the non-woven fabric is not constant and depends on the displacement, but

we can assume that its value linearly decreases by temperature in any condition. Thus we set

$$\kappa(s, T) = \kappa_{\text{fabric}}(s) \max \left(0, \frac{T_{\text{max}}^L - T}{T_{\text{max}}^L - T_0} \right).$$

Following [8], instead of a linear decreasing, a parabolic fitting with $\kappa(T) = 0$ near the fusing temperature (≈ 160 °C) can be used. Moreover, it suggests an exponential fitting for Storage modulus depending on temperature. However we used linear and parabolic fitting to maintain the model as simple as possible. Therefore

$$(4) \quad \kappa(s, T) = \kappa_{\text{fabric}}(s) \max \left(0, \frac{T_{\text{max}}^Q - T}{T_{\text{max}}^Q - T_0} \right)^2.$$

Using $\kappa(s, T)$, the force and the pressure per unit area become

$$(5) \quad P(s, T) = \frac{F(s, T)}{[\text{area}]} = \kappa(s, T)s.$$

The infinitesimal work done on the non-woven fabric (at fixed temperature) is

$$dW(s, T) = F(s, T)ds,$$

and the variation of temperature is done by the work on the fabric as follows:

$$\begin{aligned} \frac{dT(s)}{ds} &= \frac{\Delta[\text{work}]'}{C_{p,\text{fabric}}[\text{mass}]} = \frac{\frac{\Delta[\text{work}]'}{[\text{area}]}}{C_{p,\text{fabric}} \frac{[\text{mass}]}{[\text{area}]}} = \frac{F(s, T)/[\text{area}]}{C_{p,\text{fabric}} \cdot w_{\text{fabric}}} = \frac{P(s, T)}{C_{p,\text{fabric}} \cdot w_{\text{fabric}}} \\ &= \frac{\kappa(s, T)s}{C_{p,\text{fabric}} \cdot w_{\text{fabric}}}, \end{aligned}$$

where $C_{p,\text{fabric}}$ is the specific heat of the fabric. Thus, using (5), assuming that the cooling temperature negligible, the temperature increment is obtained by solving the ODE

$$(6) \quad \frac{dT(s)}{ds} = \frac{s \kappa_{\text{fabric}}(s)}{C_{p,\text{fabric}} \cdot w_{\text{fabric}}} \cdot \max \left(0, \frac{T_{\text{max}}^L - T(s)}{T_{\text{max}}^L - T_0} \right)$$

for the simple linear model, and

$$(7) \quad \frac{dT(s)}{ds} = \frac{s \kappa_{\text{fabric}}(s)}{C_{p,\text{fabric}} \cdot w_{\text{fabric}}} \cdot \max \left(0, \frac{T_{\text{max}}^Q - T(s)}{T_{\text{max}}^Q - T_0} \right)^2$$

for the parabolic interpolation model. Using the value in the table

Parameter	Value
T_0	20 °C
T_{max}^L	90 °C
T_{max}^Q	160 °C
$C_{p,\text{fabric}}$	1800 [J/(kg K)]
w_{fabric}	0.0126 [kg/m ²]

the heating (numerically) computed is plotted in the following figure

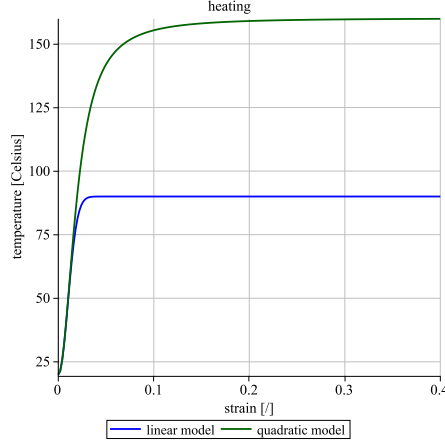


Figure 11. Heating by pressure (adiabatic case)

and a moderate strain of the compressed non-woven fabric is enough to heat up to the melting temperature.

3.5. Evaluation of the temperature decay by flux

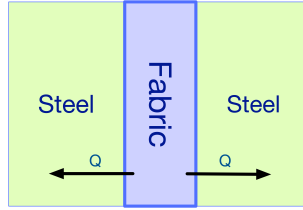


Figure 12. Heat flux

From Figure 12, assuming that the steel has fixed temperature T_{steel} , the thermal flux from the non-woven fabric to the steel using the Newton's Law of cooling is

$$Q = 2K_{\text{steel}} \frac{T_{\text{steel}} - T(t)}{h_{\text{fabric}}^{\text{min}}(1-s)/2} [\text{area}] \quad [\text{W}],$$

where K_{steel} is the thermal conductivity of the steel. The thermal conductivity and the heat capacity of the steel are very high compared to the polypropylene ones, so that they can be assumed as infinity. The temperature variation due to the heat flux using (1) becomes

$$C_{p,\text{fabric}}[\text{mass}] \frac{dT_{\text{flux}}(t)}{dt} = Q = \frac{4K_{\text{steel}}(T_{\text{steel}} - T(t))}{h_{\text{fabric}}^{\text{min}}(1-s)} [\text{area}]$$

so that

$$(8) \quad \frac{dT_{\text{flux}}(t)}{dt} = \frac{4K_{\text{steel}}(T_{\text{steel}} - T_{\text{flux}}(t))}{h_{\text{fabric}}^{\text{min}}(1-s)C_{p,\text{fabric}}[\text{mass}]/[\text{area}]} = \frac{4K_{\text{steel}}(T_{\text{steel}} - T_{\text{flux}}(t))}{h_{\text{fabric}}^{\text{min}}(1-s)C_{p,\text{fabric}}w_{\text{fabric}}}$$

assuming that the compression is done at a constant speed v [m/s]. Then we can write

$$s = \frac{v \cdot t}{h_{\text{fabric}}^{\text{min}}}$$

and

$$(9) \quad \frac{dT_{\text{flux}}(s)}{ds} \frac{v}{h_{\text{fabric}}^{\text{min}}} = \frac{4K_{\text{steel}}(T_{\text{steel}} - T_{\text{flux}}(s))}{h_{\text{fabric}}^{\text{min}}(1-s)C_{p,\text{fabric}}w_{\text{fabric}}}.$$

Using (9) with (6) or (7), we have the two complete models:

$$(10) \quad \frac{dT(s)}{ds} = \frac{s \kappa_{\text{fabric}}(s) \max\left(0, \frac{T_{\text{max}}^L - T(s)}{T_{\text{max}}^L - T_0}\right) + \frac{4K_{\text{steel}}}{v(1-s)}(T_{\text{steel}} - T(s))}{C_{p,\text{fabric}} \cdot w_{\text{fabric}}}$$

for the simple linear model, and

$$(11) \quad \frac{dT(s)}{ds} = \frac{s \kappa_{\text{fabric}}(s) \cdot \max\left(0, \frac{T_{\text{max}}^Q - T(s)}{T_{\text{max}}^Q - T_0}\right)^2 + \frac{4K_{\text{steel}}}{v(1-s)}(T_{\text{steel}} - T(s))}{C_{p,\text{fabric}} \cdot w_{\text{fabric}}}$$

for the quadratic one. We can solve numerically (10) and (11) with parameters in the next table and velocity

$$v = \frac{\Delta s}{\Delta t} = \frac{2h_{\text{fabric}}^{\min}(1-r)}{\Delta t},$$

where Δs is the size of the compression of the non-woven fabric. It is set to $h_{\text{fabric}}^{\min}(1-r)$, where r is the ratio of the fabric after the compression and the presence of the term 2 is due the the fact that the two fabric sheets are bounded. Finally Δt is the time spent through the compression.

Parameter	Value
T_0	20 °C
T_{max}^L	90 °C
T_{max}^Q	160 °C
$C_{p,\text{fabric}}$	1800 [J/(kg K)]
w_{fabric}	0.0126 [kg/m ²]
h_{fabric}^{\min}	14 μm
r	0.6
Δt	10 ms, 1 ms, 0.1 ms
K_{steel}	50 [W/(m K)]

The heating (numerically) computed is plotted in the following figure.

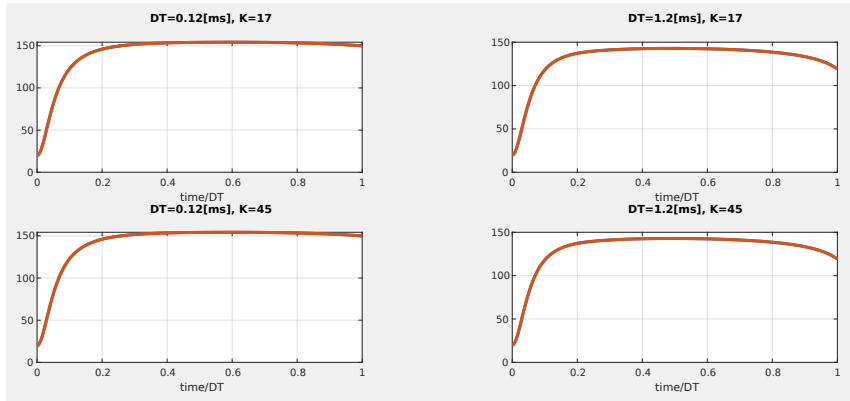


Figure 13. Heating with and without heat flux for a strain of 0.4 and a compression time of 10 ms, 1 ms and 0.1 ms, from left to right

4. The modelization of the bonding process

In this section, we model the bonding process exploited by the company to thermally bond pieces of non-woven fabric, fitting better the geometry of the steel-made rollers and their rotational velocity.

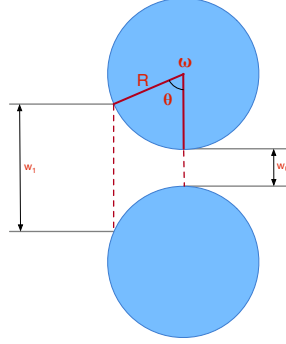


Figure 14. Compression model of two steel-made rollers

The aim of the fast compression is to reach the bounding temperature close to 150°C as noticed by other research [14,15] for Polypropylene.

4.1. Determination of the rollers velocity

Given the velocity of the non-woven fabric on the assembly line v_{fabric} (about 360 m/min, that is 6 m/s) and the ray of the rollers R (about 0.2 m), we can obtain the angular velocity of the rolls:

$$(12) \quad \omega = \frac{v_{\text{fabric}}}{R} = \frac{6 \text{ [m/s]}}{0.2 \text{ [m]}} = 30 \left[\frac{\text{rad}}{\text{s}} \right].$$

4.2. Determination of the compression angle

Looking at Figure 14 by convention, we assume that the compression starts as the non-woven fabric is compacted (that is $h_{\text{fabric}}^{\text{min}} = 14 \mu\text{m}$) neglecting the effects of the first compaction. Using d_r , the distance between the rollers, we define by

$$r = d_r / h_{\text{fabric}}^{\text{min}}$$

the compression ratio of the fabric as it is passing through the rollers. We can compute the angle θ_0 which the roller has to be subject to in order to take the non-woven fabric from thickness $h_{\text{fabric}}^{\text{min}}$ to d_r by solving:

$$h_{\text{fabric}}^{\text{min}} = d_r + 2R(1 - \cos \theta_0) = h_{\text{fabric}}^{\text{min}} r + 2R(1 - \cos \theta_0),$$

from which

$$\cos \theta_0 = 1 - \frac{h_{\text{fabric}}^{\text{min}}(1 - r)}{2R} \quad \text{or} \quad \theta_0 = \arccos \left(1 - \frac{h_{\text{fabric}}^{\text{min}}(1 - r)}{2R} \right).$$

Assuming that the angle is much small, we can Taylor approximate $\cos \theta \approx 1 - \theta^2/2$:

$$(13) \quad \theta_0 \approx \frac{\sqrt{h_{\text{fabric}}^{\text{min}}}}{\sqrt{R}} \sqrt{1 - r}.$$

For instance, using a ratio $r = 0.7$ (that is the non-woven fabric is compressed at 70% w.r.t. its starting size with $R = 0.2 \text{ m}$ and $h_{\text{fabric}}^{\text{min}} = 14 \mu\text{m}$), we obtain

$$\theta_0 \approx \frac{\sqrt{14 \cdot 10^{-6}}}{\sqrt{0.2}} \sqrt{1 - 0.7} \approx 0.004583 \text{ rad} = 0.2625 \text{ deg}.$$

4.3. Determination of the bonding time and the velocity profile

As the compression starts with $\theta(0) = -\theta_0$, the angle is changing with the law

$$(14) \quad \theta(t) = \omega t - \theta_0$$

and the thickness of the non-woven fabric does the same as follows (by Taylor approximating $\cos \theta(t)$ for small angles)

$$w(t) = h_{\text{fabric}}^{\min} r + 2R(1 - \cos \theta(t)) \Rightarrow [\text{Taylor}] \Rightarrow w(t) := h_{\text{fabric}}^{\min} r + R\theta(t)^2,$$

with compression velocity $-w'(t)$

$$-w'(t) = -2R\theta(t)\theta'(t) = 2R(\theta_0 - \omega t)\omega > 0.$$

The time to perform the bonding is given by $\omega\Delta t = \theta_0$, which for $\theta_0 = 0.004583$ rad and $\omega = 30$ rad/s gives the solution

$$\Delta t = \frac{\theta_0}{\omega} = \frac{0.004583}{30} = 0.00015275 \text{ s} = 0.15275 \text{ ms}.$$

4.4. A more accurate model for heating the non-woven fabric

By $w(t)$ and Taylor approximating the cos ($\cos \theta \approx 1 - \theta^2/2$), we can obtain the strain of the fabric w.r.t. the time $s(t)$

$$(15) \quad s(t) = 1 - \frac{w(t)}{h_{\text{fabric}}^{\min}} = 1 - \frac{h_{\text{fabric}}^{\min} r + R\theta(t)^2}{h_{\text{fabric}}^{\min}} = 1 - r - \frac{R}{h_{\text{fabric}}^{\min}} (\omega t - \theta_0)^2,$$

from which

$$(16) \quad v(t) = s'(t) = \frac{2R\omega}{h_{\text{fabric}}^{\min}} (\theta_0 - \omega t).$$

From (7), we obtain the contribution for the heating due to the compression

$$(17) \quad \begin{aligned} \frac{dT(t)}{dt} &= \frac{dT(s)}{ds} s'(t) = \frac{dT(s)}{ds} v(t) \\ &= \frac{v(t)s(t)\kappa_{\text{fabric}}(s(t))}{C_{p,\text{fabric}} \cdot w_{\text{fabric}}} \cdot \max\left(0, \frac{T_{\text{max}}^Q - T(t)}{T_{\text{max}}^Q - T_{\text{ambient}}}\right)^2, \end{aligned}$$

where $s(t)$ is given by (15) and $\kappa_{\text{fabric}}(s)$ by (3). By (8), we have the cooling law due to the touch with the steel rolls:

$$(18) \quad \frac{dT(t)}{dt} = \frac{4K_{\text{steel}}(T_{\text{steel}} - T(t))}{h_{\text{fabric}}^{\min} (1 - s(t)) C_{p,\text{fabric}} w_{\text{fabric}}}.$$

Combining the contributions of (17) and (18), we have the final model

$$(19) \quad \frac{dT(t)}{dt} = \frac{v(t)s(t)\kappa_{\text{fabric}}(s(t)) \cdot \max\left(0, \frac{T_{\text{max}}^Q - T(t)}{T_{\text{max}}^Q - T_{\text{ambient}}}\right)^2 + \frac{4K_{\text{steel}}(T_{\text{steel}} - T(t))}{h_{\text{fabric}}^{\min} (1 - s(t))}}{C_{p,\text{fabric}} w_{\text{fabric}}}.$$

In order to better compare the solutions, it is suitable to rewrite the equations in terms of the scaled time τ

$$t(\tau) = \tau\Delta t = \tau \frac{\theta_0}{\omega}$$

in such a way that

$$(20) \quad \frac{dT(\tau)}{d\tau} = \frac{dT(t(\tau))}{dt} \frac{dt(\tau)}{d\tau} = \frac{dT(t)}{dt} \frac{\theta_0}{\omega}.$$

Moreover, by (13) and (12),

$$(21) \quad \Delta t = \frac{\theta_0}{\omega} = \frac{\sqrt{R(1-r)h_{\text{fabric}}^{\min}}}{v_{\text{fabric}}}.$$

By (14), (15) and (16) together with (13), which gives $R/h_{\text{fabric}}^{\min} = (1-r)/\theta_0^2$, we have

$$(22) \quad \begin{aligned} \theta(\tau) &= \omega t - \theta_0 = (\tau - 1)\theta_0, \\ s(\tau) &= 1 - r - \frac{R}{h_{\text{fabric}}^{\min}}(\tau - 1)^2\theta_0^2 = (1-r)(1 - (\tau - 1)^2) = (1-r)\tau(2 - \tau), \\ v(\tau) &= \frac{2R\omega}{h_{\text{fabric}}^{\min}}(1 - \tau)\theta_0 = \frac{2}{\theta_0}\omega(1-r)(1 - \tau), \end{aligned}$$

from which $s(0) = 0$, $s(1) = 1 - r$ and $1 - s(\tau) = 1 - (1-r)\tau(2 - \tau)$. Moreover $v(0) = 2\sqrt{R(1-r)/h_{\text{fabric}}^{\min}}$ and $v(1) = 0$. Using (21) with (20) and (19), we obtain

$$(23) \quad \frac{dT(\tau)}{d\tau} = \frac{\theta_0}{\omega} \frac{v s \kappa_{\text{fabric}}(s) \cdot \max\left(0, \frac{T_{\text{max}}^Q - T(\tau)}{T_{\text{max}}^Q - T_{\text{ambient}}}\right)^2 + \frac{4K_{\text{steel}}(T_{\text{steel}} - T(\tau))}{h_{\text{fabric}}^{\min}(1-s)}}{C_{p,\text{fabric}}w_{\text{fabric}}}.$$

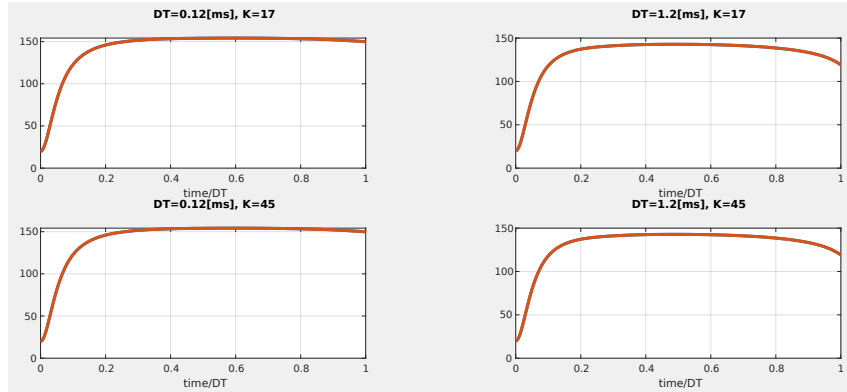


Figure 15. Heating for a strain of 0.4

4.5. Parabolic model

In order to enhance the compression of the fusing process, we consider a section (along z) of the two pieces of non-woven fabric which pass through the rollers (seen as a unique piece of non-woven fabric which is compressed). Neglecting the heat diffusion along the directions x and y (the horizontal ones), since we are assuming that the temperature gradient along such directions is small, we obtain the parabolic equation of the temperature variation (heat equation)

$$(24) \quad w_{\text{fabric}}C_{p,\text{fabric}} \frac{\partial T(t, z)}{\partial t} = K_{\text{fabric}} \frac{\partial^2 T(t, z)}{\partial z^2} + Q(t, z),$$

for $z \in (-h(t), h(t))$, where $h(t) = (1 - s(t))h_{\text{fabric}}^{\min}$, and $s(t)$ is the strain as a function of the time given by (16); the boundary conditions are given by

$$(25) \quad \begin{cases} T(0, z) = T_{\text{ambient}}, & z \in [-h_{\text{fabric}}^{\min}, h_{\text{fabric}}^{\min}] \\ T(t, -h(t)) = T(t, h(t)) = T_{\text{steel}}, & t \in [0, \Delta t] \\ \frac{\partial T(t, -h(t))}{\partial x} = \frac{\partial T(t, h(t))}{\partial x} = 0, & t \geq \Delta t \end{cases}$$

where Δt is given by (21). The production of the heat $\mathcal{Q}(t, z)$ is due to the pressure on the non-woven fabric and, as a function of the strain, is given by the r.h.s. of (17) scaled on the thickness of the fabric $2h(t) = 2(1 - s(t))h_{\text{fabric}}^{\min}$ and supposed as homogeneous (is not depending on z) along the thickness:

$$(26) \quad \mathcal{Q}(t, z) = \begin{cases} \frac{v(t)s(t)\kappa_{\text{fabric}}(s(t))}{2h(t)} \max\left(0, \frac{T_{\text{max}}^{\mathcal{Q}} - T(t, z)}{T_{\text{max}}^{\mathcal{Q}} - T_{\text{ambient}}}\right)^2, & t \leq \Delta t \\ 0, & t > \Delta t \end{cases}$$

where, by (15) and (16), we have

$$(27) \quad s(t) = \begin{cases} 1 - r - \frac{R}{h_{\text{fabric}}^{\min}}(\omega t - \theta_0)^2, & t \in [0, \Delta t] \\ 1 - r, & t \geq \Delta t \end{cases}$$

$$(28) \quad v(t) = \frac{R}{h_{\text{fabric}}^{\min}} \begin{cases} \theta_0 - \omega t, & t \in [0, \Delta t] \\ 0, & t \geq \Delta t. \end{cases}$$

Changing the time in a scaled instant $t = \tau\Delta t$ and $z \in [-h(t), h(t)]$ in $[-1, 1]$, i.e. $z = \zeta h(t)$, we obtain the re-scaled equation

$$(29) \quad h(\tau)w_{\text{fabric}}C_{p,\text{fabric}}\frac{\partial T(\tau, \zeta)}{\partial \tau} = \Delta t \left(K_{\text{fabric}} \frac{\partial^2 T(\tau, \zeta)}{\partial^2 \zeta} + \bar{\mathcal{Q}}(\tau, \zeta) \right),$$

where (using (22)), we have

$$(30) \quad \begin{aligned} \bar{\mathcal{Q}}(\tau, \zeta) &= \begin{cases} \frac{v(\tau)s(\tau)\kappa_{\text{fabric}}(s(\tau))}{2} \max\left(0, \frac{T_{\text{max}}^{\mathcal{Q}} - T(\tau, \zeta)}{T_{\text{max}}^{\mathcal{Q}} - T_{\text{ambient}}}\right)^2, & \tau \leq 1 \\ 0, & \tau > 1 \end{cases} \\ s(\tau) &= (1 - r)\tau(2 - \tau), \\ v(\tau) &= \frac{2}{\theta_0}\omega(1 - r)(1 - \tau), \\ h(\tau) &= h_{\text{fabric}}^{\min} (1 - (1 - r)\tau(2 - \tau)), \end{aligned}$$

and the boundary conditions become

$$(31) \quad \begin{cases} T(0, \zeta) = T_{\text{ambient}}, & z \in [-1, 1] \\ T(\tau, -1) = T(\tau, 1) = T_{\text{steel}}, & \tau \in [0, 1] \\ \frac{\partial T(\tau, -1)}{\partial \zeta} = \frac{\partial T(\tau, 1)}{\partial \zeta} = 0, & \tau \geq 1. \end{cases}$$

Using a spatial discretization $\Delta\zeta = 2/N$ and $\zeta_k = -1 + k\Delta\zeta$, we sample the temperature along the points ζ_k with the functions $T_k(\tau) \approx T(\tau, \zeta_k)$ for which, after the discretization, we obtain an ODE system for $\tau \leq 1$

$$(32) \quad \begin{cases} T'_0(\tau) = 0, \\ T'_k(\tau) = \Delta t \frac{(K_{\text{fabric}}/(h(\tau)\Delta\zeta^2))(T_{k-1}(\tau) - 2T_k(\tau) + T_{k+1}(\tau)) + \bar{Q}_k(\tau)}{w_{\text{fabric}}C_{p,\text{fabric}}}, \\ T'_N(\tau) = 0, \\ \bar{Q}_k(\tau) = \frac{v(\tau)s(\tau)\kappa_{\text{fabric}}(s(\tau))}{2} \max\left(0, \frac{T_{\text{max}}^Q - T_k(\tau)}{T_{\text{max}}^Q - T_{\text{ambient}}}\right)^2, \end{cases}$$

and one for $\tau \geq 0$

$$(33) \quad \begin{cases} T'_0(\tau) = \frac{\Delta t K_{\text{fabric}}}{\Delta\zeta^2 h(\tau) w_{\text{fabric}} C_{p,\text{fabric}}} (T_1(\tau) - T_0(\tau)), \\ T'_k(\tau) = \frac{\Delta t K_{\text{fabric}}}{\Delta\zeta^2 h(\tau) w_{\text{fabric}} C_{p,\text{fabric}}} (T_{k-1}(\tau) - 2T_k(\tau) + T_{k+1}(\tau)), \\ T'_N(\tau) = \frac{\Delta t K_{\text{fabric}}}{\Delta\zeta^2 h(\tau) w_{\text{fabric}} C_{p,\text{fabric}}} (T_{N-1}(\tau) - T_N(\tau)). \end{cases}$$

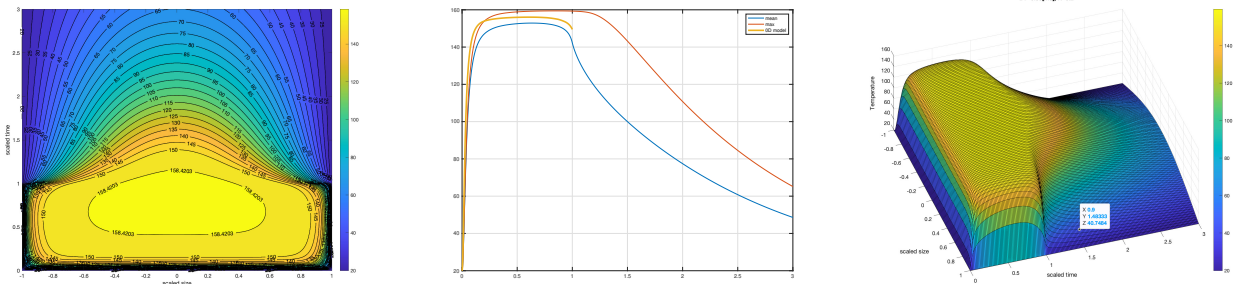


Figure 16. Solution with the parabolic model and standard parameters: $K_{\text{steel}} = 17 \text{ W}/(\text{m K})$, $v_{\text{fabric}} = 6 \text{ m/s}$ and $r = 0.8$. Estimated outgoing homogeneous temperature of $25 - 55 \text{ }^\circ\text{C}$.

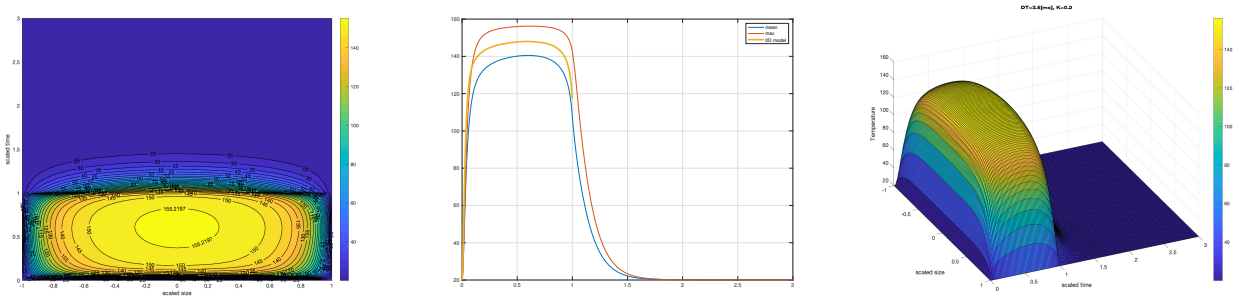


Figure 17. Solution with the parabolic model and slow scrolling: $K_{\text{steel}} = 17 \text{ W}/(\text{m K})$, $v_{\text{fabric}} = 0.6 \text{ m/s}$ and $r = 0.8$

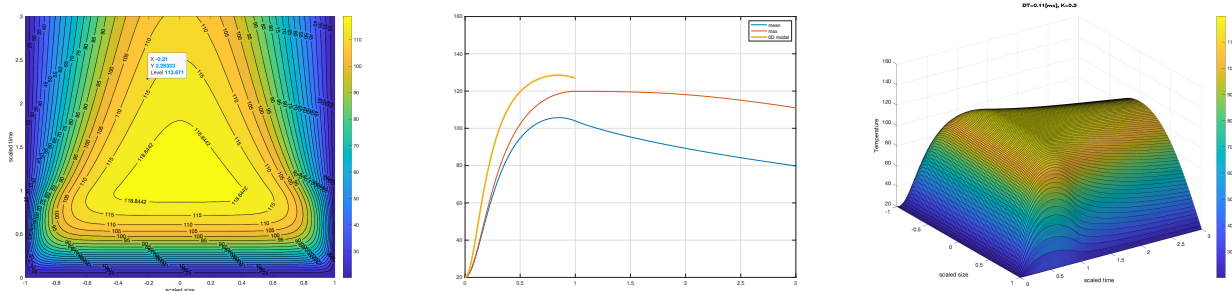


Figure 18. Solution with the parabolic model with lower compression: $K_{\text{steel}} = 17 \text{ W}/(\text{m K})$, $v_{\text{fabric}} = 6 \text{ m/s}$ and $r = 0.95$.

References

1. D. C. Cumbers, Non-woven fabrics, *World Intellectual Property Organization*, 1977.
2. R. A. Maugans, Thermally bonded fabrics and method of making same, *World Intellectual Property Organization*, 2002.
3. Y. Cengel, M. Boles, and M. Kanoglu, *Thermodynamics: An Engineering Approach*. McGraw Hill, 2023.
4. L. Formaggia, F. Saleri, and A. Veneziani, *Solving Numerical PDEs: Problems, Applications, Exercises*. Springer, 2005.
5. A. Dorigato, M. Brugnara, G. Giacomelli, L. Fambri, and A. Pegoretti, Thermal and mechanical behavior of innovative melt-blown fabrics based on polyamide nanocomposites, *Journal of Industrial Textiles*, vol. 45, no. 6, pp. 1504–1515, 2014.
6. E. Passaglia and H. K. Kevorkian, Specific heat of atactic and isotactic polypropylene and the entropy of the glass, *Journal of Applied Physics*, vol. 34, no. 1, pp. 90–97, 1963.
7. C. Maier and T. Calafut, *Polypropylene: The Definitive User's Guide and Databook*. Elsevier Science, 1998.
8. J. Li, Z. Zhu, T. Li, X. Peng, S. Jiang, and L.-S. Turng, Quantification of the young's modulus for polypropylene: Influence of initial crystallinity and service temperature, *Journal of Applied Polymer Science*, vol. 137, no. 16, p. 48581, 2020.
9. G. Gianotti and A. Capizzi, Fusion enthalpy and entropy of isotactic polypentene-1 from calorimetric measurements, *European Polymer Journal*, vol. 4, pp. 677–683, Dec. 1968.
10. V. D. E. (Ed.), *A Handbook for Materials Research and Engineering, Volume 1: Fundamentals*. Springer-Verlag Berlin, Heidelberg and Verlag Stahleisen, 1992.
11. V. D. E. (Ed.), *A Handbook for Materials Research and Engineering, Volume 2: Applications*. Springer-Verlag Berlin, Heidelberg and Verlag Stahleisen, 1993.
12. R. J. Fruehan and D. H. Wakelin, *The Making, Shaping, and Treating of Steel (11th ed.)*. Pittsburgh, PA: AISE Steel Foundation, 1998.
13. K. Bugayev, Y. Kononov, Y. Bychkov, E. Tretyakov, and I. V. Savin, *Iron and Steel Production*. The Minerva Group, Inc., 2001.
14. R. R. Hegde, G. S. Bhat, and R. A. Campbell, Thermal bonding of polypropylene films and fibers, *Journal of Applied Polymer Science*, vol. 110, pp. 3047–3058, Sept. 2008.
15. G. S. Bhat, P. K. Jangala, and J. E. Spruiell, Thermal bonding of polypropylene nonwovens: Effect of bonding variables on the structure and properties of the fabrics, *Journal of Applied Polymer Science*, vol. 92, pp. 3593–3600, Mar. 2004.